

Simplified Cofactor Conditions for Cubic to Tetragonal, Orthorhombic, and Monoclinic Phase Transformations

Hanlin Gu^{a,*} and Fan Feng^{a,†}

^aDepartment of Mechanics and Engineering Science, College of Engineering, Peking University, Beijing 100871, China.

Abstract

Cofactor Conditions (CCs) are geometric compatibility conditions mathematically derived from the crystallographic theory of martensitic phase transformation. The CCs guarantee compatible interfaces between the austenite and the parallelled twin of the martensite with any volume fraction, yielding a wide range of microstructures during phase transformation. In recent times, CCs have demonstrated tremendous applications in the rational design of low hysteresis/fatigue shape memory alloys and shape memory ceramics. In this paper, we present a simplified form of the CCs for Type I/II twins using the eigenspace of transformation stretch tensor and twin axes. We further show the explicit forms and visualizations of the simplified CCs for Cubic to Tetragonal, Cubic to Orthorhombic, and Cubic to Monoclinic I/II phase transformations. The simplified form has revealed a more straightforward correlation between the lattice parameters and the CCs, and thus provides a more convenient tool for the rational design of phase-transforming materials.

Contents

1	Introduction	2
2	Preliminaries on Twins and Cofactor Conditions	3
2.1	Type I/II Twins	3
2.2	Cofactor Conditions (CCs)	4
3	Simplified Cofactor Conditions	6
4	Visualization of the CCs in the Cubic to Tetragonal, Orthorhombic, and Monoclinic I/II Transformation	9
4.1	Cubic to Tetragonal Transformation	9
4.2	Cubic to Orthorhombic Transformation	10
4.3	Cubic to Monoclinic I Transformation	12
4.4	Cubic to Monoclinic II Transformation	14
5	Discussion	16

*Email: hanlin_gu@pku.edu.cn

†Email: fanfeng@pku.edu.cn

1 Introduction

The martensitic transformation is a first-order solid to solid diffusionless transformation, which is characterized by a sudden change in the material’s crystal structure and properties induced by the change of temperature [1], stress [2], an electric field [3, 4], or a magnetic field [5]. The martensitic phase transformation can be found in Shape Memory Materials (SMMs). SMMs are of great interest as functional materials due to the significant changes in their multiple properties during the martensitic phase transformation. They are widely used for actuation in medical devices [6, 7], micro- and nano-electro-mechanical systems (MEMS/NEMS) [8] owing to their ability to recover original shape from large deformation. Moreover, they are used for heat absorption in the development of next generation solid-state air conditioner [9–12], or energy conversion devices [13] because of their latent heat effect. Thanks to the multifunctionality of the phase transformation, active research in ferroelectric [14], ferromagnetic [15, 16], and shape magnetic [17] materials is becoming increasingly important. Therefore, developing theories that can facilitate the discovery of low fatigue (hysteresis) SMMs holds significant importance for their applications.

In the past two decades, to investigate low thermal and mechanical hysteresis SMMs for cyclic applications, strong geometric compatibility conditions, namely *Cofactor Conditions* (CCs) have been developed. When the CCs are satisfied, the SMMs can form infinite number of compatible interfaces during phase transformation, minimizing the damage caused by the mismatch of the interface between the austenite and martensite. The CCs consist of three conditions, including two equality equations and one inequality equation. Upon satisfying the first equality equation ($\lambda_2 = 1$), researchers have developed diverse low thermal hysteresis shape memory alloys (SMAs) [1, 18–27] and shape memory ceramics (SMCs) [28–31]. When all the CCs are fulfilled, two SMAs that exhibit low hysteresis in both thermal and mechanical cyclic tests [23, 24] have been discovered. The CCs serve as a powerful tool for the rational design of low fatigue SMMs and present a promising direction for the development of novel SMMs. The geometric compatibility method can also be applied to the design of origami structures [32–34], and the liquid crystal elastomers [35]. The compatible interfaces, which are studied from various perspectives including the austenite/martensite interface, foldable interface in origami structure, domain formations in ferromagnetic materials, have a great influence on materials science, engineering and artistic design.

In this paper, we propose a simplified form of the CCs in order to discover SMAs that can satisfy the CCs and exhibit large plateau strain. We initially investigate the well developed alloy systems where λ_2 is already close to 1 [1, 22, 24, 27, 36]. Furthermore, we have simplified the tensor-formed CCs into a more straightforward form using the eigenspace of the transformation stretch tensor and the twin axes of Type I/II twins. The simplified CCs form can be easily visualized and understood. We have found that the potential SMAs capable of satisfying the CCs and exhibiting large plateau strain are those undergo a Cubic to Monoclinic I/II phase transformation, rather than Cubic to Tetragonal or Cubic to Orthorhombic phase transformation.

The structure of this paper is as follows. In Section 2, we introduce the Type I/II twins and the CCs. Section 3 presents the simplified form of the CCs for Type I/II twins. Subsequently, in Section 4, we illustrate the explicit form and provide a visualization of the simplified CCs for the Cubic to Tetragonal, Cubic to Orthorhombic, and Cubic to Monoclinic I/II phase transformations. Finally, Section 5 concludes the paper and discusses the problems that yet to be studied.

2 Preliminaries on Twins and Cofactor Conditions

The martensitic phase transformation is a diffusionless transformation that occurs by the rearrangement of atoms in the crystal lattice. The high temperature phase is referred to as austenite, while the low temperature phase is known as martensite. The transformation is also accompanied by a change in the lattice parameters. And the presence of twin defects [37], crossing twins [38] triple junctions [30, 39] is frequently observed within the martensite microstructures. To comprehensively understand the geometric compatibility of the twin structure, in this section, we present an introduction of the Type I/II twins and a concise derivation of the CCs.

2.1 Type I/II Twins

The deformation gradient that maps the austenite lattice to the martensite lattice is known as the transformation stretch tensor \mathbf{U}_i , which is a symmetric positive definite matrix. Different martensite variants are characterized by distinct \mathbf{U}_i . The number of the martensite variants, denoted as n , is given by the ratio of the number of elements in the Laue group of the austenite (\mathcal{L}^a) and the number of elements in the Laue group of the martensite (\mathcal{L}^m).

A *twin* is a planar defect in the crystal and satisfies the following two properties [40]: The lattice on one side can be obtained by a simple shear or a rotation of the lattice on the other side. The kinematic compatibility condition of a twin can be formulated in the form of Equation (1) and is called *twinning equation*:

$$\mathbf{R}\mathbf{U}_j - \mathbf{U}_i = \mathbf{a} \otimes \mathbf{n}, \quad (1)$$

where $\mathbf{R} \in SO(3)$ and \mathbf{n} is the normal vector of the interface between the two deformation gradient crossing the twin interface \mathbf{U}_i and $\mathbf{R}\mathbf{U}_j$. In a twin, there are three elements that are the *twinning shear* $s = |\mathbf{a}|/|\mathbf{U}_i^{-1}\mathbf{n}|$, the *direction of shear* $\eta = \mathbf{a}/|\mathbf{a}|$, and the *shearing plane* or *twin plane* $K = \mathbf{U}_i^{-1}\mathbf{n}/|\mathbf{U}_i^{-1}\mathbf{n}|$. For the twinning equation, there exist two solutions when the middle eigenvalue of the matrix $\mathbf{C} = (\mathbf{R}\mathbf{U}_j\mathbf{U}_i^{-1})^\top(\mathbf{R}\mathbf{U}_j\mathbf{U}_i^{-1}) = \mathbf{U}_i^{-1}\mathbf{U}_j^2\mathbf{U}_i^{-1}$ equals one [41]. In the following, we will introduce the Type I and Type II twin solutions for the twinning equation.

Type I/II Twin Solutions

From the Laue group relationship of the two phases, the martensite variants are related by Equation (2)

$$\mathbf{U}_j = \mathbf{Q}\mathbf{U}_i\mathbf{Q}^\top, \quad \mathbf{Q} \in \mathcal{L}^a \setminus \mathcal{L}^m, \quad i, j \in \{1, 2, \dots, n\}. \quad (2)$$

Here, $\mathbf{Q} \in \mathcal{L}^a \setminus \mathcal{L}^m$ represents rotations that belong to the Laue group of the austenite phase (\mathcal{L}^a) but not to the Laue group of the martensite phase (\mathcal{L}^m). Equation (2) indicates that if one of the transformation stretch tensor \mathbf{U}_i is determined, all of the martensite variants \mathbf{U}_j are determined by the symmetry correlation between the austenite lattice and the martensite lattice. Since all the variants are symmetry related, the eigenvalues of the variants are the same. And the eigenvectors are related by $\mathbf{v}_k^j = \mathbf{Q}\mathbf{v}_k^i$, where \mathbf{v}_k^i is the corresponding eigenvector of the k^{th} eigenvalue λ_k for the variant \mathbf{U}_i , and $i, j \in \{1, 2, \dots, n\}$, $k \in \{1, 2, 3\}$.

When $\mathbf{U}_i \neq \mathbf{U}_j$ and $\mathbf{Q} = -\mathbf{I} + 2\hat{\mathbf{e}} \otimes \hat{\mathbf{e}}$ (a 180° rotation about the axis $\hat{\mathbf{e}}$, where $|\hat{\mathbf{e}}| = 1$), according to Mallard's Law, the two twinning solutions for a twin can be written as

$$\mathbf{a}^{\text{I}} = 2\left(\frac{\mathbf{U}_i^{-1}\hat{\mathbf{e}}}{|\mathbf{U}_i^{-1}\hat{\mathbf{e}}|^2} - \mathbf{U}_i\hat{\mathbf{e}}\right), \quad \mathbf{n}^{\text{I}} = \hat{\mathbf{e}}, \quad (3a)$$

$$\mathbf{a}^{\text{II}} = \rho\mathbf{U}_i\hat{\mathbf{e}}, \quad \mathbf{n}^{\text{II}} = \frac{2}{\rho}\left(\hat{\mathbf{e}} - \frac{\mathbf{U}_i^2\hat{\mathbf{e}}}{|\mathbf{U}_i\hat{\mathbf{e}}|^2}\right). \quad (3b)$$

Equation (3a) indicates that the *twinning plane* is a plane of symmetry in the austenite phase and is thus *rational*. This type of twin is called a *Type I twin*. Meanwhile, Equation (3b) shows that the *shearing direction* is a direction of symmetry in the austenite that is *rational*, and this is referred to as a *Type II twin* [40].

2.2 Cofactor Conditions (CCs)

Further, let's consider the interface \mathbf{m} between the austenite and the twined martensite as shown in Figure 1. Equation (1) is the compatibility equation for the paralleled twin.

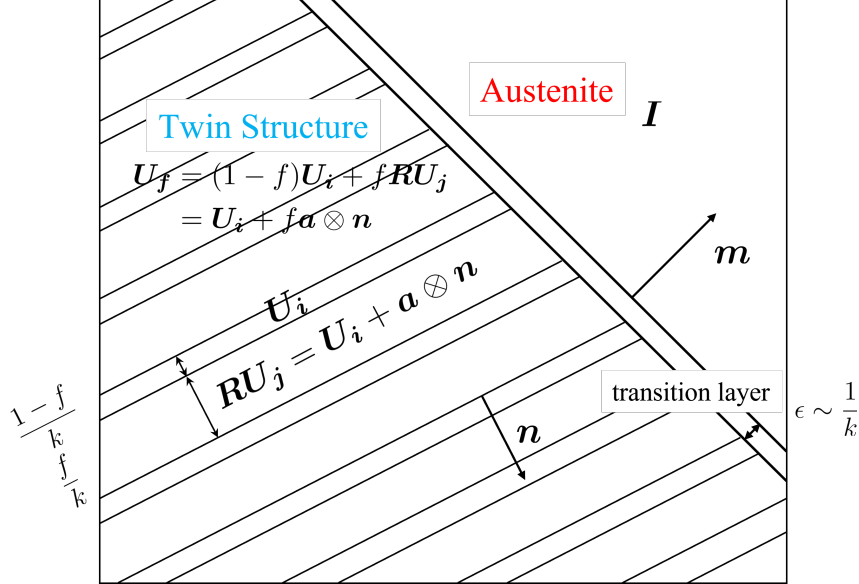


Figure 1: Schematic plot of the austenite and twined martensite interface.

The volume fraction of the two variants \mathbf{U}_i and $\mathbf{R}\mathbf{U}_j$ is $1 - f$ and f respectively, with $0 \leq f \leq 1$. Thus, the average deformation gradient of the paralleled twin microstructure is given by

$$\begin{aligned} \mathbf{U}_f &= (1 - f)\mathbf{U}_i + f\mathbf{R}\mathbf{U}_j, \\ &= \mathbf{U}_i + f\mathbf{a} \otimes \mathbf{n}. \end{aligned} \quad (4)$$

Since the interface of the parallel twin is compatible with the austenite only on average, an elastic transition layer with a thickness ϵ , on the order of $1/k$, exists. Here, $1/k$ represents the width of a single laminate composed of \mathbf{U}_i and $\mathbf{R}\mathbf{U}_j$. Consequently, as $k \rightarrow \infty$, the elastic energy of the transition layer approaches zero, which characterizes the fine-scale laminate microstructure.

The compatibility equation of the austenite and the twin microstructure is given as

$$\mathbf{R}_f \mathbf{U}_f - \mathbf{I} = \mathbf{b} \otimes \mathbf{m}. \quad (5)$$

Equation (5) has solutions if and only if \mathbf{C}_f has middle eigenvalue equal to 1, where \mathbf{C}_f can be written as

$$\begin{aligned} \mathbf{C}_f &= (\mathbf{R}_f \mathbf{U}_f)^\top (\mathbf{R}_f \mathbf{U}_f) \\ &= (\mathbf{U}_i + f\mathbf{n} \otimes \mathbf{a})(\mathbf{U}_i + f\mathbf{a} \otimes \mathbf{n}). \end{aligned} \quad (6)$$

To guarantee a compatible interface between the austenite and the twin microstructure, the necessary and sufficient conditions are

$$\det(\mathbf{C}_f - \mathbf{I}) = 0, \quad (7a)$$

$$(1 - \lambda_{1, \mathbf{C}_f})(\lambda_{3, \mathbf{C}_f} - 1) \geq 0. \quad (7b)$$

Here, λ_{i,C_f} is the eigenvalue of C_f for $i \in \{1, 2, 3\}$, with $\lambda_{1,C_f} \leq 1 \leq \lambda_{3,C_f}$. Equation (7a) shows one of the eigenvalues of C_f equals 1. The latter Equation (7b) guarantees that it is the middle eigenvalue $\lambda_{2,C_f} = 1$.

Since ‘‘determinant’’ is rank-one affine, the function $q(f) = \det(C_f - I)$ is, in fact, a quadratic function of f with $0 \leq f \leq 1$ as shown bellow:

$$\begin{aligned} q(f) &= \det(C_f - I) \\ &= \det \mathbf{U}_i \det \left(\mathbf{U}_i - \mathbf{U}_i^{-1} + f(\mathbf{a} \otimes \mathbf{n} + \mathbf{U}_i^{-1} \mathbf{n} \otimes \mathbf{U}_i^{-1} \mathbf{a}) \right). \end{aligned} \quad (8)$$

Because $q(f)$ is a quadratic function of f and symmetric about $f = 1/2$. There are three cases in general

$$(1) \quad q(f) > 0 \text{ or } q(f) < 0 \text{ for all } f \in [0, 1] \quad (9a)$$

$$(2) \quad q(f) = 0 \text{ at } f = \{f^*, 1 - f^*\} \text{ for } f^* \in [0, 1] \quad (9b)$$

$$(3) \quad q(f) = 0 \text{ for all } f \in [0, 1] \quad (9c)$$

Equation (9a) indicates no compatible interface between the austenite and the twin microstructure. A typical example is iron, which transforms from body-centered cubic (BCC) to face-centered cubic (FCC) crystal. There exists large elastic bulk energy in the transition layer and further causes dislocations, slips [42]. Thus, the functional fatigue is significant for such materials. Equation (9b) depicts a typical scenario for SMMs where a finite number, specifically 4, of compatible interface can be formed. For the equation $q(f) = 0$, there exists two solutions for the volume fraction, denoted as f^* and $1 - f^*$. If Equation (7b) is also satisfied, then for each of these volume fraction solutions, there are two corresponding twin solutions [41]. Therefore, in total, four austenite/laminate interfaces m per twin system exhibit geometric compatibility.

Equation (9c) indicates that for any volume fraction $f \in [0, 1]$, $q(f) = 0$, which means the elastic energy is zero for all f . This leads to the existence of an infinite number of zero elastic energy interfaces. When integrated with Equation (7b), the strong geometric compatibility conditions for the interface between the austenite and twined martensite can be derived. These conditions are denoted as the *Cofactor Conditions (CCs)* [18, 22], which are presented in the following:

$$\begin{aligned} \lambda_2 &= 1 && \text{CC1,} \\ \mathbf{a} \cdot \mathbf{U}_i \text{ cof}(\mathbf{U}_i^2 - I) \mathbf{n} &= 0 && \text{CC2,} \\ \text{tr } \mathbf{U}_i^2 - \det \mathbf{U}_i^2 - \frac{\mathbf{a}^2 \mathbf{n}^2}{4} - 2 &\geq 0 && \text{CC3.} \end{aligned} \quad (10)$$

Here, λ_2 is the middle eigenvalue of \mathbf{U}_i . And \mathbf{a} and \mathbf{n} are twinning equation solutions.

Derivation of CCs

Equation (9c) makes the quadratic function $q(f)$ identically equal to 0, which is equivalent to $q(0) = 0$ and $q'(0) = 0$. By direction calculation [41], we have

$$g(0) = \det(\mathbf{U}_i^2 - I) = 0 \quad (11a)$$

$$g'(0) = 2\mathbf{a} \cdot \mathbf{U}_i \text{ cof}(\mathbf{U}_i^2 - I) \mathbf{n} = 0 \quad (11b)$$

Here, ‘‘cof’’ denotes the cofactor matrix. Equation (11a) can be written as

$$\det(\mathbf{U}_i^2 - I) = (\lambda_1^2 - 1)(\lambda_2^2 - 1)(\lambda_3^2 - 1) = 0,$$

which implies one of the eigenvalue of \mathbf{U}_i equals 1. When $f = 0$, the twin microstructure degenerates into a pure variant. Therefore, the eigenvalue that equal to one has to be the middle eigenvalue of \mathbf{U}_i . Then, the condition $\lambda_2 = 1$ is denoted as *CC1*. Equation (11b) guarantees that the parallel twin with any volume fraction f is compatible with the austenite. Hence, *CC2* is expressed as

$$\mathbf{a} \cdot \mathbf{U}_i \text{ cof}(\mathbf{U}_i^2 - I) \mathbf{n} = 0. \quad (12)$$

Although Equation (11a) and (11b) ensure that one of the eigenvalue of \mathbf{C}_f is equal to 1, they do not guarantee that this eigenvalue is the middle one. Equation (7b) is necessary to ensure that the eigenvalue equal to 1 is indeed the middle eigenvalue of \mathbf{C}_f . We know that

$$\begin{aligned} & (1 - \lambda_{1,\mathbf{C}_f})(\lambda_{3,\mathbf{C}_f} - 1) \\ &= (\lambda_{1,\mathbf{C}_f} + 1 + \lambda_{3,\mathbf{C}_f}) - \lambda_{1,\mathbf{C}_f}\lambda_{3,\mathbf{C}_f} - 2 \\ &= \text{tr } \mathbf{C}_f - \det \mathbf{C}_f - 2. \end{aligned} \quad (13)$$

The expression can be formulated in terms of the stretch tensor \mathbf{U}_i and twinning solutions as presented below:

$$\begin{aligned} \text{tr } \mathbf{C}_f &= \text{tr } \mathbf{U}_i^2 + (f^2 - f)|\mathbf{a}|^2|\mathbf{n}|^2, \\ \det \mathbf{C}_f &= \det \mathbf{U}_i^2, \end{aligned}$$

The detailed derivation is provided in the Appendix. Hence, we get

$$\begin{aligned} & (1 - \lambda_{1,\mathbf{C}_f})(\lambda_{3,\mathbf{C}_f} - 1) \\ &= \text{tr } \mathbf{U}_i^2 + (f^2 - f)|\mathbf{a}|^2|\mathbf{n}|^2 - \det \mathbf{U}_i^2 - 2 \geq 0. \end{aligned} \quad (14)$$

To guarantee that Equation (14) is true for all volume fractions, a stronger condition, denoted as $CC3$, is represented as follows:

$$\text{tr } \mathbf{U}_i^2 - \det \mathbf{U}_i^2 - \frac{1}{4}|\mathbf{a}|^2|\mathbf{n}|^2 - 2 \geq 0. \quad (15)$$

This is because the minimum value of the function $(f^2 - f) = -1/4$ for $0 \leq f \leq 1$. Therefore, Equation (14) holds true for all volume fractions.

The CCs are more than a mathematical result, they serve as the theoretical guidance for the development of low fatigue martensitic phase transformation materials. By tuning the SMAs to closely satisfy the CCs, researchers have successfully discovered the alloys $\text{Zn}_{45}\text{Au}_{30}\text{Cu}_{25}$ [23, 43] and $\text{Ti}_{54.7}\text{Ni}_{30.7}\text{Cu}_{12.3}\text{Co}_{2.3}$ [24]. These two cofactor alloys, $\text{Zn}_{45}\text{Au}_{30}\text{Cu}_{25}$ and $\text{Ti}_{54.7}\text{Ni}_{30.7}\text{Cu}_{12.3}\text{Co}_{2.3}$, have demonstrated extremely low hysteresis during both thermal and mechanical cycling. Specifically, a $\text{Zn}_{45}\text{Au}_{30}\text{Cu}_{25}$ nanopillar has been shown to endure 10^5 reversible compression cycles [45], and a $\text{Ti}_{54.7}\text{Ni}_{30.7}\text{Cu}_{12.3}\text{Co}_{2.3}$ thin film can withstand 10^7 reversible tensile cycles [24].

3 Simplified Cofactor Conditions

In this section, we introduce a novel form of the CCs relevant to Type I/II twins. To fulfill the CCs, the two equalities and one inequality presented in Equation (10) must be satisfied simultaneously. We assume that the first equality, $\lambda_2 = 1$, holds true. In Type I/II twins, the twin variants are related by 180° rotations. These rotations give rise to a particular solution form for the twinning equation, as shown in Equation (3). Further, CC2 and CC3 will be formulated in terms of the twin solutions corresponding to Type I/II twins. This newly simplified version of the CCs is presented in Equation (17). To derive this form of the CCs, we simplify the tensor-formed CCs using the eigenspace of the transformation stretch tensor \mathbf{U}_i and the Type I/II twin axes $\hat{\mathbf{e}}$.

First, we represent \mathbf{U}_i in the context of its eigenspace as

$$\mathbf{U}_i = \lambda_1 \mathbf{v}_1 \otimes \mathbf{v}_1 + \lambda_2 \mathbf{v}_2 \otimes \mathbf{v}_2 + \lambda_3 \mathbf{v}_3 \otimes \mathbf{v}_3. \quad (16)$$

Here, for $i \in \{1, 2, 3\}$, λ_i denotes the eigenvalues of \mathbf{U}_i , and \mathbf{v}_i represents corresponding eigenvectors associated with λ_i . The eigenvalues are labelled such that $0 < \lambda_1 \leq \lambda_2 \leq \lambda_3$. We further present the CCs in a simplified form by substituting the eigenspace of \mathbf{U}_i and the twinning solutions of Type I/II twins into the CCs.

Theorem 3.1. *The simplified CCs for Type I and Type II twins can be expressed as follows:*

$$\text{Type I Twin: } \begin{cases} \lambda_2 = 1 & \text{CC1,} \\ \lambda_3^2(\mathbf{v}_1 \cdot \hat{\mathbf{e}})^2 + \lambda_1^2 \lambda_3^2 (\mathbf{v}_2 \cdot \hat{\mathbf{e}})^2 + \lambda_1^2 (\mathbf{v}_3 \cdot \hat{\mathbf{e}})^2 - \lambda_1^2 \lambda_3^2 = 0 & \text{CC2,} \\ \lambda_1^2 + \lambda_2^2 - \lambda_1^2 \lambda_3^2 - \lambda_1^2 (\mathbf{v}_1 \cdot \hat{\mathbf{e}})^2 - (\mathbf{v}_2 \cdot \hat{\mathbf{e}})^2 - \lambda_3^2 (\mathbf{v}_3 \cdot \hat{\mathbf{e}})^2 \geq 0 & \text{CC3,} \end{cases} \quad (17a)$$

$$\text{Type II Twin: } \begin{cases} \lambda_2 = 1 & \text{CC1,} \\ \lambda_1^2 (\mathbf{v}_1 \cdot \hat{\mathbf{e}})^2 + (\mathbf{v}_2 \cdot \hat{\mathbf{e}})^2 + \lambda_3^2 (\mathbf{v}_3 \cdot \hat{\mathbf{e}})^2 - 1 = 0 & \text{CC2,} \\ \lambda_1^2 + \lambda_3^2 - \lambda_1^2 \lambda_3^2 - \lambda_1^4 (\mathbf{v}_1 \cdot \hat{\mathbf{e}})^2 - (\mathbf{v}_2 \cdot \hat{\mathbf{e}})^2 - \lambda_3^4 (\mathbf{v}_3 \cdot \hat{\mathbf{e}})^2 \geq 0 & \text{CC3.} \end{cases} \quad (17b)$$

Proof. First, we assume that CC1 ($\lambda_2 = 1$) is satisfied. The terms below can be further simplified as

$$\begin{aligned} (a) \quad & \mathbf{U}_i^2 - \mathbf{I} = (\lambda_1^2 - 1)\mathbf{v}_1 \otimes \mathbf{v}_1 + (\lambda_3^2 - 1)\mathbf{v}_3 \otimes \mathbf{v}_3 \\ & \Rightarrow \text{cof}(\mathbf{U}_i^2 - \mathbf{I}) = (\lambda_1^2 - 1)(\lambda_3^2 - 1)\mathbf{v}_2 \otimes \mathbf{v}_2, \\ (b) \quad & \text{tr} \mathbf{U}_i^2 = \lambda_1^2 + \lambda_3^2 + 1, \\ (c) \quad & \det \mathbf{U}_i^2 = \lambda_1^2 \lambda_3^2. \end{aligned} \quad (18)$$

Type I Twins

Substituting the twinning solutions of Type I twin as in Equation (3a) into the CC2, we have the following:

$$\begin{aligned} & \mathbf{a} \cdot \mathbf{U}_i \text{cof}(\mathbf{U}_i^2 - \mathbf{I})\mathbf{n} \\ & = 2 \left(\frac{\mathbf{U}_i^{-1}\hat{\mathbf{e}}}{|\mathbf{U}_i^{-1}\hat{\mathbf{e}}|^2} - \mathbf{U}_i\hat{\mathbf{e}} \right) \cdot \mathbf{U}_i \text{cof}(\mathbf{U}_i^2 - \mathbf{I})\hat{\mathbf{e}}, \\ & = 2 \left(\frac{1}{|\mathbf{U}_i^{-1}\hat{\mathbf{e}}|^2} \hat{\mathbf{e}} \cdot \text{cof}(\mathbf{U}_i^2 - \mathbf{I})\hat{\mathbf{e}} - \hat{\mathbf{e}} \cdot \mathbf{U}_i^2 \text{cof}(\mathbf{U}_i^2 - \mathbf{I})\hat{\mathbf{e}} \right). \end{aligned} \quad (19)$$

Since $\mathbf{U}_i^2 = \lambda_1^2 \mathbf{v}_1 \otimes \mathbf{v}_1 + \mathbf{v}_2 \otimes \mathbf{v}_2 + \lambda_3^2 \mathbf{v}_3 \otimes \mathbf{v}_3$, and $\text{cof}(\mathbf{U}_i^2 - \mathbf{I}) = (\lambda_1^2 - 1)(\lambda_3^2 - 1)\mathbf{v}_2 \otimes \mathbf{v}_2$, we have

$$\mathbf{U}_i^2 \text{cof}(\mathbf{U}_i^2 - \mathbf{I}) = (\lambda_1^2 - 1)(\lambda_3^2 - 1)\mathbf{v}_2 \otimes \mathbf{v}_2.$$

Therefore, CC2 = 0 can be written as

$$(\lambda_1^2 - 1)(\lambda_3^2 - 1) \left(\frac{1}{|\mathbf{U}_i^{-1}\hat{\mathbf{e}}|^2} - 1 \right) |\hat{\mathbf{e}} \cdot \mathbf{v}_2|^2 = 0. \quad (20)$$

Equation (20) indicates that there are special conditions under which CC2 is automatically satisfied. When $\hat{\mathbf{e}} \cdot \mathbf{v}_2 = 0$, the equation above is always true. Nevertheless, this situation arises from the symmetry relationship rather than the material properties, and they cannot be valid for all twins. Therefore, it is regarded as a trivial case. Further, the *simplified CC2 of Type I twin* is given as

$$\begin{aligned} & |\mathbf{U}_i^{-1}\hat{\mathbf{e}}|^2 - 1 = 0 \\ & \Rightarrow \frac{1}{\lambda_1^2} (\mathbf{v}_1 \cdot \hat{\mathbf{e}})^2 + (\mathbf{v}_2 \cdot \hat{\mathbf{e}})^2 + \frac{1}{\lambda_3^2} (\mathbf{v}_3 \cdot \hat{\mathbf{e}})^2 - 1 = 0, \\ & \Rightarrow \lambda_3^2 (\mathbf{v}_1 \cdot \hat{\mathbf{e}})^2 + \lambda_1^2 \lambda_3^2 (\mathbf{v}_2 \cdot \hat{\mathbf{e}})^2 + \lambda_1^2 (\mathbf{v}_3 \cdot \hat{\mathbf{e}})^2 - \lambda_1^2 \lambda_3^2 = 0. \end{aligned} \quad (21)$$

To simplify the CC3, we express $|\mathbf{a}|^2$ and $|\mathbf{n}|^2$ in relation to \mathbf{U}_i and $\hat{\mathbf{e}}$ as

$$\begin{aligned} |\mathbf{a}|^2 & = 4 \left(\frac{\mathbf{U}_i^{-1}\hat{\mathbf{e}}}{|\mathbf{U}_i^{-1}\hat{\mathbf{e}}|^2} - \mathbf{U}_i\hat{\mathbf{e}} \right) \cdot \left(\frac{\mathbf{U}_i^{-1}\hat{\mathbf{e}}}{|\mathbf{U}_i^{-1}\hat{\mathbf{e}}|^2} - \mathbf{U}_i\hat{\mathbf{e}} \right), \\ & = 4 \left(\frac{1 - 2\hat{\mathbf{e}} \cdot \hat{\mathbf{e}}}{|\mathbf{U}_i^{-1}\hat{\mathbf{e}}|^2} + |\mathbf{U}_i\hat{\mathbf{e}}|^2 \right), \\ & = 4(|\mathbf{U}_i\hat{\mathbf{e}}|^2 - 1), \\ |\mathbf{n}|^2 & = |\hat{\mathbf{e}}|^2 = 1. \end{aligned}$$

Thus, the CC3 is expressed as

$$\begin{aligned} & \text{tr } \mathbf{U}_i^2 - \det \mathbf{U}_i^2 - \frac{|\mathbf{a}|^2 |\mathbf{n}|^2}{4} - 2 \\ &= \lambda_1^2 + \lambda_3^2 - \lambda_1^2 \lambda_3^2 - |\mathbf{U}_i \hat{\mathbf{e}}|^2 \geq 0. \end{aligned}$$

And, it is easy to know that

$$|\mathbf{U}_i \hat{\mathbf{e}}|^2 = \lambda_1^2 (\mathbf{v}_1 \cdot \hat{\mathbf{e}})^2 + (\mathbf{v}_2 \cdot \hat{\mathbf{e}})^2 + \lambda_3^2 (\mathbf{v}_3 \cdot \hat{\mathbf{e}})^2.$$

Finally, the *simplified CC3 of Type I twin* is given as

$$\lambda_1^2 + \lambda_2^2 - \lambda_1^2 \lambda_3^2 - \lambda_1^2 (\mathbf{v}_1 \cdot \hat{\mathbf{e}})^2 - (\mathbf{v}_2 \cdot \hat{\mathbf{e}})^2 - \lambda_3^2 (\mathbf{v}_3 \cdot \hat{\mathbf{e}})^2 \geq 0. \quad (22)$$

Type II twins

Substituting the twinning solutions of Type II twin, as represented in Equation (3b), into the CC2, the following result is obtained:

$$\begin{aligned} & \mathbf{a} \cdot \mathbf{U}_i \text{ cof } (\mathbf{U}_i^2 - \mathbf{I}) \mathbf{n} \\ &= 2 \left(\hat{\mathbf{e}} \cdot \mathbf{U}_i^2 \text{ cof } (\mathbf{U}_i^2 - \mathbf{I}) \hat{\mathbf{e}} - \hat{\mathbf{e}} \cdot \mathbf{U}_i^2 \text{ cof } (\mathbf{U}_i^2 - \mathbf{I}) \mathbf{U}_i^2 \frac{\hat{\mathbf{e}}}{|\mathbf{U}_i \hat{\mathbf{e}}|^2} \right). \end{aligned}$$

Based on Equation (18) and the condition $\lambda_2 = 1$, it is obvious that

$$\mathbf{U}_i^2 \text{ cof } (\mathbf{U}_i^2 - \mathbf{I}) \mathbf{U}_i^2 = (\lambda_1^2 - 1)(\lambda_3^2 - 1) \mathbf{v}_2 \otimes \mathbf{v}_2$$

Therefore, the CC2 can be simplified as

$$(\lambda_1^2 - 1)(\lambda_3^2 - 1) \left(1 - \frac{1}{|\mathbf{U}_i \hat{\mathbf{e}}|^2}\right) |\hat{\mathbf{e}} \cdot \mathbf{v}_2|^2 = 0 \quad (23)$$

Avoiding the trivial case that $\hat{\mathbf{e}} \cdot \mathbf{v}_2 = 0$, the *simplified CC2 for Type II twin* is

$$\begin{aligned} & |\mathbf{U}_i \hat{\mathbf{e}}|^2 - 1 = 0 \\ & \Rightarrow \lambda_1^2 (\mathbf{v}_1 \cdot \hat{\mathbf{e}})^2 + (\mathbf{v}_2 \cdot \hat{\mathbf{e}})^2 + \lambda_3^2 (\mathbf{v}_3 \cdot \hat{\mathbf{e}})^2 - 1 = 0 \end{aligned} \quad (24)$$

Similarly, to simple the CC3 of Type II twin, we note that the first two CCs, $\lambda_2 = 1$ (CC1) and $|\mathbf{U}_i \hat{\mathbf{e}}|^2 = 1$ (CC2), hold true. From this, we can derive the following results:

$$\begin{aligned} & |\mathbf{a}|^2 = \mathbf{a} \cdot \mathbf{a} = |\mathbf{U}_i \hat{\mathbf{e}}|^2 = 1, \\ & |\mathbf{n}|^2 = 4 \left(\hat{\mathbf{e}} - \frac{\mathbf{U}_i^2 \hat{\mathbf{e}}}{|\mathbf{U}_i \hat{\mathbf{e}}|^2} \right) \cdot \left(\hat{\mathbf{e}} - \frac{\mathbf{U}_i^2 \hat{\mathbf{e}}}{|\mathbf{U}_i \hat{\mathbf{e}}|^2} \right) \\ &= 4 \left(1 - \frac{\mathbf{U}_i^T \hat{\mathbf{e}} \cdot \mathbf{U}_i \hat{\mathbf{e}} + \mathbf{U}_i \hat{\mathbf{e}} \cdot \mathbf{U}_i^T \hat{\mathbf{e}}}{|\mathbf{U}_i \hat{\mathbf{e}}|^2} + |\mathbf{U}_i^2 \hat{\mathbf{e}}|^2 \right) \\ &= 4(|\mathbf{U}_i^2 \hat{\mathbf{e}}|^2 - 1). \end{aligned}$$

Therefore, CC3 can be expressed as

$$\begin{aligned} & \text{tr } \mathbf{U}_i^2 - \det \mathbf{U}_i^2 - \frac{|\mathbf{a}|^2 |\mathbf{n}|^2}{4} - 2 \\ &= \lambda_1^2 + \lambda_3^2 - \lambda_1^2 \lambda_3^2 - |\mathbf{U}_i^2 \hat{\mathbf{e}}|^2 \geq 0. \end{aligned}$$

By substituting the following expression into the above equation,

$$|\mathbf{U}_i^2 \hat{\mathbf{e}}|^2 = \lambda_1^4 (\mathbf{v}_1 \cdot \hat{\mathbf{e}})^2 + (\mathbf{v}_2 \cdot \hat{\mathbf{e}})^2 + \lambda_3^4 (\mathbf{v}_3 \cdot \hat{\mathbf{e}})^2.$$

we obtain that the *simplified CC3 of Type II twin*, which is represented as

$$\lambda_1^2 + \lambda_3^2 - \lambda_1^2 \lambda_3^2 - \lambda_1^4 (\mathbf{v}_1 \cdot \hat{\mathbf{e}})^2 - (\mathbf{v}_2 \cdot \hat{\mathbf{e}})^2 - \lambda_3^4 (\mathbf{v}_3 \cdot \hat{\mathbf{e}})^2 \geq 0. \quad (25)$$

□

The simplified CCs are expressed in terms of the eigenspace of the transformation stretch tensor \mathbf{U}_i , and the twin axes of the Type I/II twins. For a specific martensitic phase transformation, the key lies in finding the eigenspace decomposition of \mathbf{U}_i and the twin relationship among the martensite variants. The simplified CCs provide a clear and simple way for verifying the CCs. They are more intuitive and easier to understand than the tensor form. Moreover, the simplified form is convenient for visualizing the satisfaction of the CCs.

4 Visualization of the CCs in the Cubic to Tetragonal, Orthorhombic, and Monoclinic I/II Transformation

4.1 Cubic to Tetragonal Transformation

Theorem 4.1. *In the Cubic to Tetragonal transformation, the CCs cannot be exactly satisfied.*

Proof. The materials with Cubic to Tetragonal transformation have 3 variants [40] of martensite and are given as

$$\mathbf{U}_1 = \begin{pmatrix} \alpha & 0 & 0 \\ 0 & \alpha & 0 \\ 0 & 0 & \beta \end{pmatrix}, \quad \mathbf{U}_2 = \begin{pmatrix} \alpha & 0 & 0 \\ 0 & \beta & 0 \\ 0 & 0 & \alpha \end{pmatrix}, \quad \mathbf{U}_3 = \begin{pmatrix} \beta & 0 & 0 \\ 0 & \alpha & 0 \\ 0 & 0 & \alpha \end{pmatrix}, \quad (26)$$

where $\alpha = \frac{a}{a_0}$, and $\gamma = \frac{a}{a_0}$. a_0 is the lattice parameter of the cubic phase, and a, c are the lattice parameters of the tetragonal phase.

CC1 implies $\lambda_2 = \alpha = 1$ and $\lambda_{1 \text{ or } 3} = \beta \neq 1$. In the SMMs, typically the tetragonal c -axis is elongated and plane perpendicular to c -axis is compressed. That is, $\alpha < 1$ and $\beta > 1$. The eigenspace becomes $\mathbf{U}_i = \mathbf{v}_1 \otimes \mathbf{v}_1 + \mathbf{v}_2 \otimes \mathbf{v}_2 + \beta \mathbf{v}_3 \otimes \mathbf{v}_3$.

As the fact that $\mathbf{U}_i^2 - \mathbf{I} = (\beta^2 - 1)\mathbf{v}_3 \otimes \mathbf{v}_3$,

$$\text{cof}(\mathbf{U}_i^2 - \mathbf{I}) = \mathbf{0}.$$

Hence, CC2 = $\mathbf{a} \cdot \mathbf{U}_i \text{cof}(\mathbf{U}_i^2 - \mathbf{I})\mathbf{n} = 0$ is automatically satisfied. This means that one of the eigenvalue of \mathbf{C}_f in Equation (6) is always equal to 1. However, CC3 is always not satisfied as shown below:

$$\begin{aligned} \text{CC3} &= \text{tr} \mathbf{U}_i^2 - \det \mathbf{U}_i^2 - \frac{|\mathbf{a}|^2 |\mathbf{n}|^2}{4} - 2, \\ &= 2 + \beta^2 - \beta^2 - \frac{|\mathbf{a}|^2 |\mathbf{n}|^2}{4} - 2, \\ &= -\frac{|\mathbf{a}|^2 |\mathbf{n}|^2}{4} \leq 0. \end{aligned} \quad (27)$$

The direct calculation of $(1 - \lambda_{1, \mathbf{C}_f})(\lambda_{3, \mathbf{C}_f} - 1)$ as in Equation (14) shows that

$$\begin{aligned} &\text{tr} \mathbf{U}_i^2 + (f^2 - f)|\mathbf{a}|^2 |\mathbf{n}|^2 - \det \mathbf{U}_i^2 - 2 \\ &= (1 + 1 + \beta^2) + (f^2 - f)|\mathbf{a}|^2 |\mathbf{n}|^2 - \beta^2 - 2 \\ &= (f^2 - f)|\mathbf{a}|^2 |\mathbf{n}|^2 \geq 0. \end{aligned}$$

The equation above is valid only at $f = 0$ or $f = 1$ which suggests if the pure variant forms compatible interface with the austenite, then the laminated twins are always not compatible. \square

In the experiments, it is hard to find SMMs undergoing Cubic to Tetragonal transformation with $\lambda_2 = 1$. However, attempts have been made to tune the λ_2 close to 1, and the modified CCs has been studied [29].

4.2 Cubic to Orthorhombic Transformation

There are various SMA systems such as CuAlNi [44], NiTiCu/Pd/Au/Pt [1, 19, 24] has B2 (Cubic) to B19 (Orthorhombic) phase transformation.

Theorem 4.2. *The simplified CCs of Type I/II twins for Cubic to Orthorhombic transformation represent a segment of a curve in (λ_1, λ_3) space. The expression are presented as follows:*

$$\text{Type I Twin: } \begin{cases} \lambda_2 = 1 & \text{CC1,} \\ \lambda_1^2 + 2\lambda_3^2 - 3\lambda_1^2\lambda_3^2 = 0 \Rightarrow \lambda_3 = \frac{\lambda_1}{\sqrt{3\lambda_1^2 - 2}} & \text{CC2,} \\ 2\lambda_1^2 + 3\lambda_3^2 - 4\lambda_1^2\lambda_3^2 - 1 \geq 0 & \text{CC3,} \end{cases} \quad (28a)$$

$$\text{Type II Twin: } \begin{cases} \lambda_2 = 1 & \text{CC1,} \\ 2\lambda_1^2 + \lambda_3^2 - 3 = 0 \Rightarrow \lambda_3 = \sqrt{3 - 2\lambda_1^2} & \text{CC2,} \\ -2\lambda_1^4 - \lambda_3^4 - 4\lambda_1^2\lambda_3^2 + 4(\lambda_1^2 + \lambda_3^2) - 1 \geq 0 & \text{CC3.} \end{cases} \quad (28b)$$

Proof. In the Cubic to Orthorhombic transformation, there are $24/4 = 6$ variants of martensite as

$$\begin{aligned} \mathbf{U}_1 &= \begin{pmatrix} \beta & 0 & 0 \\ 0 & \frac{\alpha + \gamma}{2} & \frac{\alpha - \gamma}{2} \\ 0 & \frac{\alpha - \gamma}{2} & \frac{\alpha + \gamma}{2} \end{pmatrix}, & \mathbf{U}_2 &= \begin{pmatrix} \beta & 0 & 0 \\ 0 & \frac{\alpha + \gamma}{2} & \frac{-\alpha + \gamma}{2} \\ 0 & \frac{-\alpha + \gamma}{2} & \frac{\alpha + \gamma}{2} \end{pmatrix}, \\ \mathbf{U}_3 &= \begin{pmatrix} \frac{\alpha + \gamma}{2} & 0 & \frac{\alpha - \gamma}{2} \\ 0 & \beta & 0 \\ \frac{\alpha - \gamma}{2} & 0 & \frac{\alpha + \gamma}{2} \end{pmatrix}, & \mathbf{U}_4 &= \begin{pmatrix} \frac{\alpha + \gamma}{2} & 0 & \frac{-\alpha + \gamma}{2} \\ 0 & \beta & 0 \\ \frac{-\alpha + \gamma}{2} & 0 & \frac{\alpha + \gamma}{2} \end{pmatrix}, \\ \mathbf{U}_5 &= \begin{pmatrix} \frac{\alpha + \gamma}{2} & \frac{\alpha - \gamma}{2} & 0 \\ \frac{\alpha - \gamma}{2} & \frac{\alpha + \gamma}{2} & 0 \\ 0 & 0 & \beta \end{pmatrix}, & \mathbf{U}_6 &= \begin{pmatrix} \frac{\alpha + \gamma}{2} & \frac{-\alpha + \gamma}{2} & 0 \\ \frac{-\alpha + \gamma}{2} & \frac{\alpha + \gamma}{2} & 0 \\ 0 & 0 & \beta \end{pmatrix}. \end{aligned} \quad (29)$$

where,

$$\alpha = \frac{a}{\sqrt{2}a_0}, \quad \beta = \frac{b}{a_0}, \quad \gamma = \frac{c}{\sqrt{2}a_0},$$

and a_0 represents the lattice parameter of the cubic phase, while a, b, c denotes the orthorhombic lattice parameters. With out loss of generality, let

$$\mathbf{U}_i = \mathbf{U}_1 = \begin{pmatrix} \beta & 0 & 0 \\ 0 & \frac{\alpha + \gamma}{2} & \frac{\alpha - \gamma}{2} \\ 0 & \frac{\alpha - \gamma}{2} & \frac{\alpha + \gamma}{2} \end{pmatrix}$$

Concerning Type I/II twins, our focus is restricted to rotations within the Laue group of the cubic crystal structure that correspond to a 180° rotation. There exist nine rotations $\mathbf{Q}_{[\hat{e}, 180^\circ]}$, where \hat{e} belongs to the set $\{\mathbf{e}_1, \mathbf{e}_2, \mathbf{e}_3, \mathbf{e}_4, \mathbf{e}_5, \mathbf{e}_6, \mathbf{e}_7, \mathbf{e}_8, \mathbf{e}_9\}$. These rotations are listed as follows:

$$\begin{aligned} \mathbf{e}_1 &= [1, 0, 0], & \mathbf{e}_2 &= [0, 1, 0], & \mathbf{e}_3 &= [0, 0, 1], \\ \mathbf{e}_4 &= \frac{1}{\sqrt{2}}[1, 1, 0], & \mathbf{e}_5 &= \frac{1}{\sqrt{2}}[1, \bar{1}, 0], & \mathbf{e}_6 &= \frac{1}{\sqrt{2}}[0, 1, 1], \\ \mathbf{e}_7 &= \frac{1}{\sqrt{2}}[0, 1, \bar{1}], & \mathbf{e}_8 &= \frac{1}{\sqrt{2}}[1, 0, 1], & \mathbf{e}_9 &= \frac{1}{\sqrt{2}}[1, 0, \bar{1}]. \end{aligned} \quad (30)$$

The eigenspace of $\mathbf{U}_i = \lambda_1 \mathbf{v}_1 \otimes \mathbf{v}_1 + \lambda_2 \mathbf{v}_2 \otimes \mathbf{v}_2 + \lambda_3 \mathbf{v}_3 \otimes \mathbf{v}_3$ is given as follows:

$$\begin{cases} \lambda_1 = \beta, & \mathbf{v}_1 = [1, 0, 0], \\ \lambda_2 = \alpha, & \mathbf{v}_2 = [0, 1, 1], \\ \lambda_3 = \gamma, & \mathbf{v}_3 = [0, \bar{1}, 1]. \end{cases} \quad (31)$$

When the 180^{circ} rotation axis $\hat{\mathbf{e}}$ is parallel to any eigenvector \mathbf{v}_i , the two variants \mathbf{U}_i and \mathbf{U}_j are identical, thus they can no longer form twin structures. Therefore, there is no need to discuss the cases in which $\hat{\mathbf{e}} \times \mathbf{v}_i = (0, 0, 0)$. It is evident that $\mathbf{e}_1 \parallel \mathbf{v}_1$, $\mathbf{e}_6 \parallel \mathbf{v}_2$ and $\mathbf{e}_7 \parallel \mathbf{v}_3$. For the set $\hat{\mathbf{e}} = \{\mathbf{e}_2, \mathbf{e}_3\}$, as they form compound twins, there is no further discussion regarding them. Consequently, the 180° rotations axes considered in the simplified CCs for Cubic to Orthogonal transformation are limited to the following four axes:

$$\hat{\mathbf{e}} \in \{\mathbf{e}_4, \mathbf{e}_5, \mathbf{e}_8, \mathbf{e}_9\}. \quad (32)$$

By substituting the eigenspace and rotation axes into the simplified CCs for Type I/II twins are presented in Equation (17a) and (17b), in Cubic to Orthorhombic phase transformation, CC2 and CC3 are further expressed as functions of λ_1 and λ_3 , as shown in Equation (28a), and (28b). It can be further demonstrated that by the satisfaction of CC1 and CC2 in Cubic to Orthorhombic transformation, CC3 is automatically satisfied. \square

The results above suggest that for Type I/II twins in Cubic to Orthorhombic phase transformation, the CCs are essentially a segment of a curve composed of variables λ_1 and λ_3 as in Figure 2. In the figure, the red curve represents the CC2 for Type I twin,

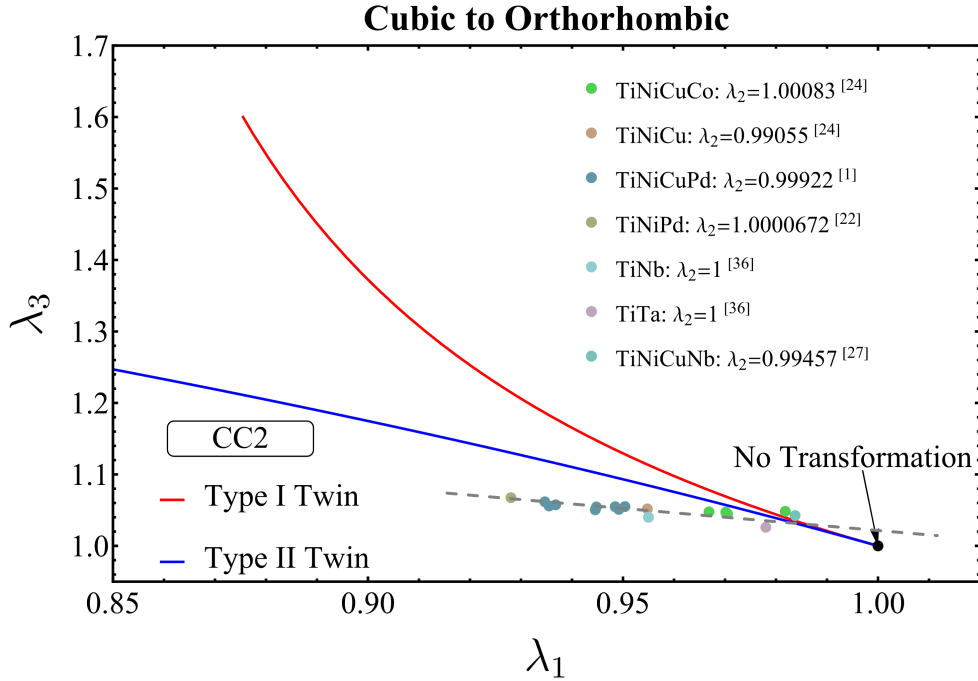


Figure 2: Simplified CCs in Cubic to Orthorhombic phase transformation for $\lambda_2 = 1$. The colored points represents the SMAs that have λ_2 near 1 [1, 22, 24, 27, 36].

and the blue curve represents the CC2 for Type II twin. The colored dots represent the SMAs with λ_2 close to 1. Specifically, the green dots for $\text{Ti}_{54.7}\text{Ni}_{30.7}\text{Cu}_{12.3}\text{Co}_{2.3}$ are plotted bases on the in-situ X-ray diffraction data acquired during the stress-induced transformation. These dots are very close to CC2 curves and intersect them during the transition process. This result is consistent with the numerical calculation of the CCs, which indicates that $\text{Ti}_{54.7}\text{Ni}_{30.7}\text{Cu}_{12.3}\text{Co}_{2.3}$ closely satisfies the CCs [24]. However, the plateau strain is only approximately 1%. The superelasticity of SMAs is of interest for a

plenty of applications, which generally requires the plateau strain to be greater than 5%. To achieve a large plateau strain, we search for materials with larger values of $|\lambda_1 - 1|$ and $|\lambda_3 - 1|$ among the dotted materials in Figure 2. Surprisingly, the dashed line indicates that the dotted materials are restricted by an unknown mechanism, making it almost impossible to tune the SMAs with Cubic to Orthorhombic transformation to both satisfy the CCs and achieve large plateau strain. However, the cofactor alloy $\text{Zn}_{45}\text{Au}_{30}\text{Cu}_{25}$ is shown to exhibit approximately 6% plateau strain in the nanopillar compression test and endure 10^5 cycles [45]. This finding motivates the exploration of the Cubic to Monoclinic phase transformation. From a crystallographic perspective, the only difference between orthorhombic crystal and monoclinic crystal lies in the angle between a - and c -axis of the martensite. To search for reversible martensitic transformation materials with large plateau strain, we further investigate the Cubic to Monoclinic I/II Transformation in Section 4.3, and 4.4.

4.3 Cubic to Monoclinic I Transformation

In the Cubic to Monoclinic phase transformation, there are two distinct ways [46, 47], which are called Cubic to Monoclinic I/II depending on their 2-fold monoclinic b -axis. In the following, we will discuss the simplified CCs for the Cubic to Monoclinic I/II transformation separately. In the Cubic to Monoclinic I transformation, the monoclinic I lattice has a unique 2-fold axis along a face-diagonal of the parent-phase, so that the variants are called “face-diagonal” variants.

Theorem 4.3. *The simplified CCs of Type I/II twins for the Cubic to Monoclinic I transformation are two sets of solution given as follows:*

$$(1) \hat{e} \in \left\{ \mathbf{e}_4 = \frac{1}{\sqrt{2}}[1, 1, 0], \mathbf{e}_8 = \frac{1}{\sqrt{2}}[1, 0, 1] \right\}$$

Type I Twin:

$$\begin{cases} \lambda_2 = 1 & \text{CC1,} \\ 3(\lambda_1^2 + \lambda_3^2) - 6\lambda_1^2\lambda_3^2 - 4\sqrt{2}\lambda_1\lambda_3 \cot \theta + \sqrt{(\lambda_1^2 + \lambda_3^2)^2 - 4\lambda_1^2\lambda_3^2 \csc^2 \theta} = 0 & \text{CC2,} \\ 5\lambda_1^2 + 5\lambda_3^2 - 8\lambda_1^2\lambda_3^2 - 4\sqrt{2}\lambda_1\lambda_3 \cot \theta + \sqrt{(\lambda_1^2 + \lambda_3^2)^2 - 4\lambda_1^2\lambda_3^2 \csc^2 \theta} - 2 \geq 0 & \text{CC3,} \end{cases} \quad (33a)$$

Type II Twin:

$$\begin{cases} \lambda_2 = 1 & \text{CC1,} \\ -6 + 3(\lambda_1^2 + \lambda_3^2) + 4\sqrt{2}\lambda_1\lambda_3 \cot \theta - \sqrt{(\lambda_1^2 + \lambda_3^2)^2 - 4\lambda_1^2\lambda_3^2 \csc^2 \theta} = 0 & \text{CC2,} \\ -3\lambda_1^4 - 8\lambda_1^2\lambda_3^2 - 3\lambda_3^4 + 8(\lambda_1^2 + \lambda_3^2) - 4\sqrt{2}(\lambda_1^2 + \lambda_3^2)\lambda_1\lambda_3 \cot \theta \\ \quad + (\lambda_1^2 + \lambda_3^2)\sqrt{(\lambda_1^2 + \lambda_3^2)^2 - 4\lambda_1^2\lambda_3^2 \csc^2 \theta} - 2 \geq 0 & \text{CC3,} \end{cases} \quad (33b)$$

$$(2) \hat{e} \in \left\{ \mathbf{e}_5 = \frac{1}{\sqrt{2}}[1, \bar{1}, 0], \mathbf{e}_9 = \frac{1}{\sqrt{2}}[1, 0, \bar{1}] \right\}$$

Type I Twin:

$$\begin{cases} \lambda_2 = 1 & \text{CC1,} \\ 3(\lambda_1^2 + \lambda_3^2) - 6\lambda_1^2\lambda_3^2 + 4\sqrt{2}\lambda_1\lambda_3 \cot \theta + \sqrt{(\lambda_1^2 + \lambda_3^2)^2 - 4\lambda_1^2\lambda_3^2 \csc^2 \theta} = 0 & \text{CC2,} \\ 5\lambda_1^2 + 5\lambda_3^2 - 8\lambda_1^2\lambda_3^2 + 4\sqrt{2}\lambda_1\lambda_3 \cot \theta + \sqrt{(\lambda_1^2 + \lambda_3^2)^2 - 4\lambda_1^2\lambda_3^2 \csc^2 \theta} - 2 \geq 0 & \text{CC3,} \end{cases} \quad (34a)$$

Type II Twin:

$$\begin{cases} \lambda_2 = 1 & \text{CC1,} \\ -6 + 3(\lambda_1^2 + \lambda_3^2) - 4\sqrt{2}\lambda_1\lambda_3 \cot \theta - \sqrt{(\lambda_1^2 + \lambda_3^2)^2 - 4\lambda_1^2\lambda_3^2 \csc^2 \theta} = 0 & \text{CC2,} \\ -3\lambda_1^4 - 8\lambda_1^2\lambda_3^2 - 3\lambda_3^4 + 8(\lambda_1^2 + \lambda_3^2) - 4\sqrt{2}(\lambda_1^2 + \lambda_3^2)\lambda_1\lambda_3 \cot \theta \\ \quad + (\lambda_1^2 + \lambda_3^2)\sqrt{(\lambda_1^2 + \lambda_3^2)^2 - 4\lambda_1^2\lambda_3^2 \csc^2 \theta} - 2 \geq 0 & \text{CC3.} \end{cases} \quad (34b)$$

Proof. In the Cubic to Monoclinic I transformation, there are $24/2 = 12$ variants of martensite [47]. The variants are given by:

$$\begin{aligned}
\mathbf{U}_1 &= \begin{pmatrix} \xi & \rho & \rho \\ \rho & \sigma & \tau \\ \rho & \tau & \sigma \end{pmatrix}, \mathbf{U}_2 = \begin{pmatrix} \xi & -\rho & -\rho \\ -\rho & \sigma & \tau \\ -\rho & \tau & \sigma \end{pmatrix}, \mathbf{U}_3 = \begin{pmatrix} \xi & -\rho & \rho \\ -\rho & \sigma & -\tau \\ \rho & -\tau & \sigma \end{pmatrix}, \mathbf{U}_4 = \begin{pmatrix} \xi & \rho & -\rho \\ \rho & \sigma & \tau \\ -\rho & \tau & \sigma \end{pmatrix}, \\
\mathbf{U}_5 &= \begin{pmatrix} \sigma & \rho & \tau \\ \rho & \xi & \rho \\ \tau & \rho & \sigma \end{pmatrix}, \mathbf{U}_6 = \begin{pmatrix} \sigma & -\rho & \tau \\ -\rho & \xi & -\rho \\ \tau & -\rho & \sigma \end{pmatrix}, \mathbf{U}_7 = \begin{pmatrix} \sigma & -\rho & -\tau \\ -\rho & \xi & \rho \\ -\tau & \rho & \sigma \end{pmatrix}, \mathbf{U}_8 = \begin{pmatrix} \sigma & \rho & -\tau \\ \rho & \xi & -\rho \\ -\tau & -\rho & \sigma \end{pmatrix}, \\
\mathbf{U}_9 &= \begin{pmatrix} \sigma & \tau & \rho \\ \tau & \sigma & \rho \\ \rho & \rho & \xi \end{pmatrix}, \mathbf{U}_{10} = \begin{pmatrix} \sigma & \tau & -\rho \\ \tau & \sigma & -\rho \\ -\rho & -\rho & \xi \end{pmatrix}, \mathbf{U}_{11} = \begin{pmatrix} \sigma & -\tau & \rho \\ -\tau & \sigma & -\rho \\ \rho & -\rho & \xi \end{pmatrix}, \mathbf{U}_{12} = \begin{pmatrix} \sigma & -\tau & -\rho \\ -\tau & \sigma & \rho \\ -\rho & \rho & \xi \end{pmatrix},
\end{aligned} \tag{35}$$

where

$$\begin{aligned}
\sigma &= \frac{1}{2} \left(\frac{\gamma(\alpha \sin(\theta) + \gamma)}{\sqrt{\alpha^2 + 2\alpha\gamma \sin(\theta) + \gamma^2}} + \beta \right), \\
\tau &= \frac{1}{2} \left(\frac{\gamma(\alpha \sin(\theta) + \gamma)}{\sqrt{\alpha^2 + 2\alpha\gamma \sin(\theta) + \gamma^2}} - \beta \right), \\
\rho &= \frac{\alpha\gamma \cos(\theta)}{\sqrt{2}\sqrt{\alpha^2 + 2\alpha\gamma \sin(\theta) + \gamma^2}}, \\
\xi &= \frac{\alpha(\alpha + \gamma \sin(\theta))}{\sqrt{\alpha^2 + 2\alpha\gamma \sin(\theta) + \gamma^2}},
\end{aligned}$$

and $\alpha = a/a_0, \beta = b/\sqrt{2}a_0, \gamma = c/\sqrt{2}a_0$. a_0 is lattice parameter of cubic lattice, a, b, c, θ are lattice parameters of monoclinic I lattice. Here, θ is the monoclinic angle between the monoclinic a - and c -axis.

Take \mathbf{U}_i as \mathbf{U}_1 , we have

$$\mathbf{U}_i = \mathbf{U}_1 = \begin{pmatrix} \xi & \rho & \rho \\ \rho & \sigma & \tau \\ \rho & \tau & \sigma \end{pmatrix}.$$

The eigenspace of $\mathbf{U}_i = \lambda_1 \mathbf{v}_1 \otimes \mathbf{v}_1 + \lambda_2 \mathbf{v}_2 \otimes \mathbf{v}_2 + \lambda_3 \mathbf{v}_3 \otimes \mathbf{v}_3$ is

$$\begin{cases} \lambda_1 = \frac{1}{2}(-\sqrt{\alpha^2 + \gamma^2 - 2\alpha\gamma \sin \theta} + \sqrt{\alpha^2 + \gamma^2 + 2\alpha\gamma \sin \theta}), \\ \lambda_2 = \beta, \\ \lambda_3 = \frac{1}{2}(\sqrt{\alpha^2 + \gamma^2 - 2\alpha\gamma \sin \theta} + \sqrt{\alpha^2 + \gamma^2 + 2\alpha\gamma \sin \theta}), \end{cases}$$

$$\begin{cases} \mathbf{e}\mathbf{v}_1 = \left[1, \frac{-\sec \theta(\alpha^2 - \gamma^2) + \sqrt{\alpha^2 + \gamma^2 - 2\alpha\gamma \sin \theta} \sqrt{\alpha^2 + \gamma^2 + 2\alpha\gamma \sin \theta}}{2\sqrt{2}\alpha\gamma}, \right. \\ \left. \frac{-\sec \theta(\alpha^2 - \gamma^2) + \sqrt{\alpha^2 + \gamma^2 - 2\alpha\gamma \sin \theta} \sqrt{\alpha^2 + \gamma^2 + 2\alpha\gamma \sin \theta}}{2\sqrt{2}\alpha\gamma} \right], \\ \mathbf{e}\mathbf{v}_2 = [0, \bar{1}, 1] \\ \mathbf{e}\mathbf{v}_3 = \left[\frac{-\sec \theta(\alpha^2 - \gamma^2) + \sqrt{\alpha^2 + \gamma^2 - 2\alpha\gamma \sin \theta} \sqrt{\alpha^2 + \gamma^2 + 2\alpha\gamma \sin \theta}}{2\sqrt{2}\alpha\gamma}, 1, 1 \right] \end{cases} \tag{36}$$

For brevity, the $\mathbf{e}\mathbf{v}_i$ above are non-normalized. The normalized eigenvectors $\mathbf{v}_i = \mathbf{e}\mathbf{v}_i/|\mathbf{e}\mathbf{v}_i|$ for $i = \{1, 2, 3\}$. Similar to the Cubic to Monoclinic I transformation, rotation axes that parallel to eigenvectors that make the variants identical are neglected. It's not hard to find that $\mathbf{e}_7 \parallel \mathbf{v}_2$. In Section 3, among the nine rotations, there are trivial cases for the simplified CCs, where $\hat{\mathbf{e}} \cdot \mathbf{v}_2 = 0$. We find that for $\hat{\mathbf{e}} = \{\mathbf{e}_1, \mathbf{e}_6\}$, the trivial condition

$\hat{\mathbf{e}} \cdot \mathbf{v}_2 = 0$ is satisfied, and these cases are also neglected. Therefore, the 180° rotation axes considered in simplified CCs for Cubic to Monoclinic I transformation are

$$\hat{\mathbf{e}} \in \{\mathbf{e}_2, \mathbf{e}_3, \mathbf{e}_4, \mathbf{e}_5, \mathbf{e}_8, \mathbf{e}_9\}. \quad (37)$$

By substituting the eigenspace and the rotation axes into the simplified CCs in Equation (17a) and (17b), we can further express CC2 and CC3 as functions of λ_1 , λ_3 , and θ , as shown in Equation (33) and (34). Note that, in Cubic to Monoclinic I transformation, the satisfaction of CC1 and CC2 also automatically implies the satisfaction of CC3. \square

The CCs of the Type I/II twins in Cubic to Monoclinic I phase transformation can be viewed in the space of $(\lambda_1, \lambda_2, \lambda_3, \theta)$ with $0 < \lambda_1 \leq \lambda_2 \leq \lambda_3$, $\theta \in [0^\circ, 180^\circ]$. It's a bounded composed of $\lambda_1, \lambda_3, \theta$ on $\lambda_2 = 1$ plane. When $\theta = 90^\circ$, it turns the monoclinic lattice into an orthorhombic lattice. The results of the simplified CCs for the Cubic to Monoclinic I transformation in Equation (33) and (34) degenerate to those of the Cubic to Orthorhombic transformation in Equation (28).

4.4 Cubic to Monoclinic II Transformation

The monoclinic II lattice has a unique 2-fold axis along an edge of the original cubic lattice, so the variants are also called ‘‘cube-edge’’ variants.

Theorem 4.4. *The simplified CCs of Type I/II twins for the Cubic to Monoclinic II transformation are two sets of solution given as follows:*

$$(1) \hat{\mathbf{e}} \in \left\{ \mathbf{e}_4 = \frac{1}{\sqrt{2}}[1, 1, 0], \mathbf{e}_5 = \frac{1}{\sqrt{2}}[1, \bar{1}, 0] \right\}$$

$$\text{Type I Twin: } \begin{cases} \lambda_2 = 1 & \text{CC1,} \\ \lambda_1^2 + 2\lambda_3^2 - 3\lambda_1^2\lambda_3^2 - 2\lambda_1^2\lambda_3 \cot \theta = 0 & \text{CC2,} \\ 2\lambda_1^2 + 3\lambda_3^2 - 4\lambda_1^2\lambda_3^2 - 2\lambda_3 \cot \theta - 1 \geq 0 & \text{CC3,} \end{cases} \quad (38a)$$

$$\text{Type II Twin: } \begin{cases} \lambda_2 = 1 & \text{CC1,} \\ -3 + 2\lambda_1^2 + \lambda_3^2 + 2\lambda_3 \cot \theta = 0 & \text{CC2,} \\ -2\lambda_1^4 - \lambda_3^4 - 4\lambda_1^2\lambda_3^2 + 4(\lambda_1^2 + \lambda_3^2) - 2(\lambda_3 + \lambda_3^3) \cot \theta - 1 \geq 0 & \text{CC3,} \end{cases} \quad (38b)$$

$$(2) \hat{\mathbf{e}} \in \left\{ \mathbf{e}_8 = \frac{1}{\sqrt{2}}[1, 0, 1], \mathbf{e}_9 = \frac{1}{\sqrt{2}}[1, 0, \bar{1}] \right\}$$

$$\text{Type I Twin: } \begin{cases} \lambda_2 = 1 & \text{CC1,} \\ \lambda_1^2 + 2\lambda_3^2 - 3\lambda_1^2\lambda_3^2 + 2\lambda_1^2\lambda_3 \cot \theta = 0 & \text{CC2,} \\ 2\lambda_1^2 + 3\lambda_3^2 - 4\lambda_1^2\lambda_3^2 + 2\lambda_3 \cot \theta - 1 \geq 0 & \text{CC3,} \end{cases} \quad (39a)$$

$$\text{Type II Twin: } \begin{cases} \lambda_2 = 1 & \text{CC1,} \\ -3 + 2\lambda_1^2 + \lambda_3^2 - 2\lambda_3 \cot \theta = 0 & \text{CC2,} \\ -2\lambda_1^4 - \lambda_3^4 - 4\lambda_1^2\lambda_3^2 + 4(\lambda_1^2 + \lambda_3^2) + 2(\lambda_3 + \lambda_3^3) \cot \theta - 1 \geq 0 & \text{CC3.} \end{cases} \quad (39b)$$

Proof. Similarly, in the Cubic to Monoclinic II transformation, the number of variants is

$24/2 = 12$ and the variants are written as [47]:

$$\begin{aligned}
\mathbf{U}_1 &= \begin{pmatrix} \beta & 0 & 0 \\ 0 & \rho & \sigma \\ 0 & \sigma & \tau \end{pmatrix}, \mathbf{U}_2 = \begin{pmatrix} \beta & 0 & 0 \\ 0 & \rho & -\sigma \\ 0 & -\sigma & \tau \end{pmatrix}, \mathbf{U}_3 = \begin{pmatrix} \beta & 0 & 0 \\ 0 & \tau & \sigma \\ 0 & \sigma & \rho \end{pmatrix}, \mathbf{U}_4 = \begin{pmatrix} \beta & 0 & 0 \\ 0 & \tau & -\sigma \\ 0 & -\sigma & \rho \end{pmatrix}, \\
\mathbf{U}_5 &= \begin{pmatrix} \rho & 0 & \sigma \\ 0 & \beta & 0 \\ \sigma & 0 & \tau \end{pmatrix}, \mathbf{U}_6 = \begin{pmatrix} \rho & 0 & -\sigma \\ 0 & \beta & 0 \\ -\sigma & 0 & \tau \end{pmatrix}, \mathbf{U}_7 = \begin{pmatrix} \tau & 0 & \sigma \\ 0 & \beta & 0 \\ \sigma & 0 & \rho \end{pmatrix}, \mathbf{U}_8 = \begin{pmatrix} \tau & 0 & -\sigma \\ 0 & \beta & 0 \\ -\sigma & 0 & \rho \end{pmatrix}, \\
\mathbf{U}_9 &= \begin{pmatrix} \rho & \sigma & 0 \\ \sigma & \tau & 0 \\ 0 & 0 & \beta \end{pmatrix}, \mathbf{U}_{10} = \begin{pmatrix} \rho & -\sigma & 0 \\ -\sigma & \tau & 0 \\ 0 & 0 & \beta \end{pmatrix}, \mathbf{U}_{11} = \begin{pmatrix} \tau & \sigma & 0 \\ \sigma & \rho & 0 \\ 0 & 0 & \beta \end{pmatrix}, \mathbf{U}_{12} = \begin{pmatrix} \tau & -\sigma & 0 \\ -\sigma & \rho & 0 \\ 0 & 0 & \beta \end{pmatrix},
\end{aligned} \tag{40}$$

where

$$\begin{aligned}
\rho &= \frac{\alpha^2 + \gamma^2 + 2\alpha\gamma(\sin(\theta) + \cos(\theta))}{2\sqrt{\alpha^2 + \gamma^2 + 2\alpha\gamma\sin(\theta)}}, \\
\sigma &= \frac{\alpha^2 - \gamma^2}{2\sqrt{\alpha^2 + \gamma^2 + 2\alpha\gamma\sin(\theta)}}, \\
\tau &= \frac{\alpha^2 + \gamma^2 + 2\alpha\gamma(\sin(\theta) - \cos(\theta))}{2\sqrt{\alpha^2 + \gamma^2 + 2\alpha\gamma\sin(\theta)}},
\end{aligned}$$

and $\beta = b/a_0$, $\alpha = \sqrt{2}a/a_0$, $\gamma \propto c/a_0$. Here, the lattice parameter of cubic lattice is a_0 and lattice parameters of monoclinic II lattice are a , b , c , and θ . The explicit form of γ depends on the unit cell of the monoclinic II lattice, which is a long-period stacking cell. Various stackings are found in a number of SMAs such as 2H, 9R, and 18R structures reported in Cu-Zn, Cu-Al-Ni, Cu-Zn-Au, Cu-Zn-Al, and Cu-Zn-Ga [23, 48, 49].

Similarly, we choose

$$\mathbf{U}_i = \mathbf{U}_1 = \begin{pmatrix} \beta & 0 & 0 \\ 0 & \rho & \sigma \\ 0 & \sigma & \tau \end{pmatrix}.$$

The eigenspace of $\mathbf{U}_i = \lambda_1 \mathbf{v}_1 \otimes \mathbf{v}_1 + \lambda_2 \mathbf{v}_2 \otimes \mathbf{v}_2 + \lambda_3 \mathbf{v}_3 \otimes \mathbf{v}_3$ is as follows:

$$\begin{cases} \lambda_1 = \beta \\ \lambda_2 = \frac{1}{2}(\rho + \tau - \sqrt{\rho^2 + 4\sigma^2 - 2\rho\tau + \tau^2}) \\ \lambda_3 = \frac{1}{2}(\rho + \tau + \sqrt{\rho^2 + 4\sigma^2 - 2\rho\tau + \tau^2}) \end{cases} \tag{41}$$

$$\begin{cases} \mathbf{e}\mathbf{v}_1 = [1, 0, 0] \\ \mathbf{e}\mathbf{v}_2 = (0, -\frac{\rho + \tau + \sqrt{\rho^2 + 4\sigma^2 - 2\rho\tau + \tau^2}}{2\sigma}, 1) \\ \mathbf{e}\mathbf{v}_3 = (0, -\frac{\rho + \tau - \sqrt{\rho^2 + 4\sigma^2 - 2\rho\tau + \tau^2}}{2\sigma}, 1) \end{cases}$$

Also, the eigenvalue $\mathbf{v}_i = \mathbf{e}\mathbf{v}_i/|\mathbf{e}\mathbf{v}_i|$ for $i = \{1, 2, 3\}$. In the Cubic to Monoclinic II transformation, $\mathbf{e}_1 \parallel \mathbf{v}_1$ gives no twin. There exists the trivial cases such that $\hat{\mathbf{e}} \cdot \mathbf{v}_2 = 0$ when $\hat{\mathbf{e}} \in \{\mathbf{e}_2, \mathbf{e}_3, \mathbf{e}_6, \mathbf{e}_7\}$. Therefore, the 180° rotation axes considered in the simplified CCs for Cubic to Monoclinic II transformation are

$$\hat{\mathbf{e}} \in \{\mathbf{e}_4, \mathbf{e}_5, \mathbf{e}_8, \mathbf{e}_9\}. \tag{42}$$

We substitute the eigenspace and the rotation axes into the simplified CCs in Equation (17), there are two solution sets for Type I/II twins, as shown in Equation (38), and (39). Unlike the previous cases, in the Cubic to Monoclinic II transformation, the satisfaction of CC1 and CC2 does not automatically imply the satisfaction of CC3. Assuming

CC1 and CC2 are satisfied, the sign of $CC3(\lambda_1, \lambda_3)$, which represents the sign of CC3 value corresponding to the first set of Type I twin solution defined in Equation (38a) is shown in Figure 3. This demonstrates that the surfaces of CC2 and CC3 intersect, and the satisfaction of CC1 and CC2 does not automatically guarantee CC3 is greater or equal to zero. \square

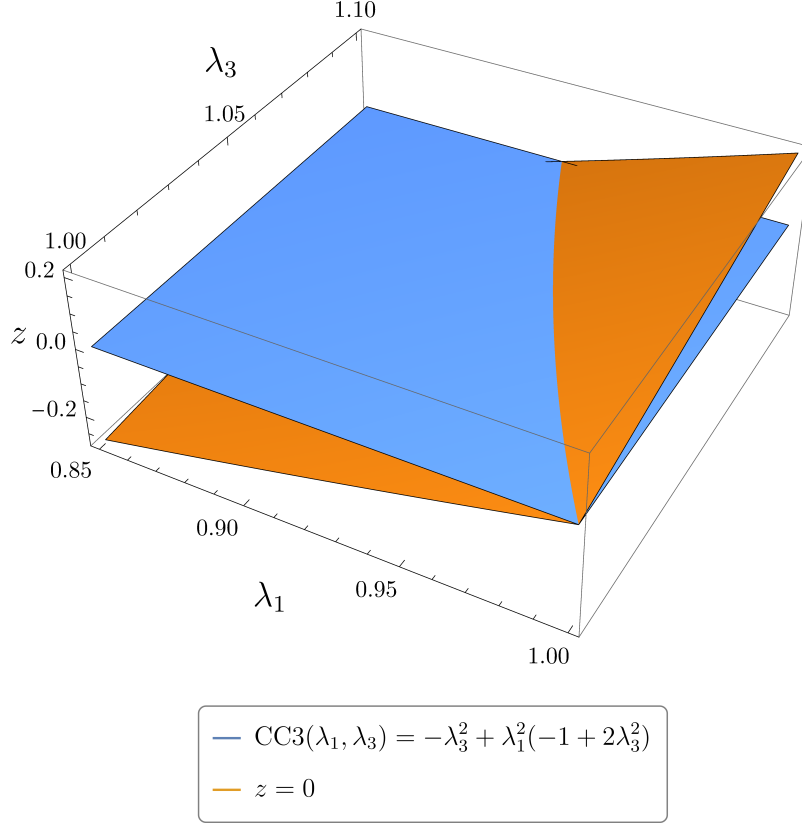


Figure 3: An example of CC3 surface in terms of λ_1 and λ_3 for the Type I twin in Cubic to Monoclinic II transformation, assuming CC1 and CC2 are satisfied.

Similar to the Cubic to Monoclinic I phase transformation, the simplified CCs of Type I/II twins in Cubic to Monoclinic II phase transformation form a bounded surface defined by $\lambda_1, \lambda_3, \theta$ on the $\lambda_2 = 1$ plane. When $\theta = 90^\circ$, the results of the simplified CCs for the Cubic to Monoclinic II transformation in Equation (38) and (39) also degenerate to those of the Cubic to Orthorhombic transformation in Equation (28).

Figure 4 shows that the $Zn_{45}Au_{30}Cu_{25}$ alloy lies almost exactly on the cofactor curve for Type II twin with its monoclinic angle of 86.80° in the case $\hat{e} \in \{e_4, e_5\}$. This figure depicts the CCs curves corresponding to various monoclinic angles. The notation θ° in “Type I/II θ° ” represents the monoclinic angle of the monoclinic lattice. The colored dots stand for materials that undergo a Cubic to Orthorhombic transformation, as shown in Figure 2. To find SMAs that satisfy the CCs with large plateau strain, we propose that by tuning the angle between the a - and c - axis of the orthorhombic lattice to deviate from 90° , the dotted materials have great potential to lie on the simplified CCs surfaces from the Cubic to Monoclinic I/II phase transformation.

5 Discussion

In this paper, we present the simplified CCs method for Type I/II twins for the martensitic phase transformation. The simplified CCs method is based on the eigenspace of the transformation stretch tensor, and the rotation axes of the Type I/II twins. The simplified

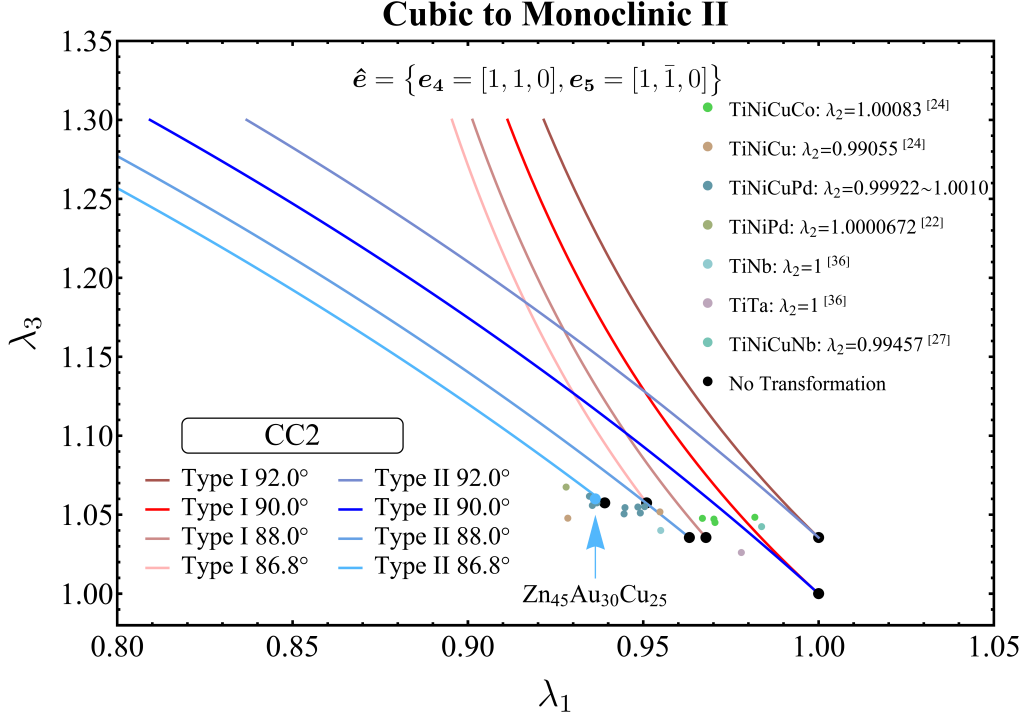


Figure 4: Visualization of the CCs in Cubic to Monoclinic II Phase Transformation for Type I/II twins, when $\hat{e} \in \left\{e_4 = \frac{1}{\sqrt{2}}[1, 1, 0], e_5 = \frac{1}{\sqrt{2}}[1, \bar{1}, 0]\right\}$.

CCs have build a direct correlation of the lattice parameters and the CCs. Compare to the direct calculation of the CCs values, the simplified form provide a more intuitive way to visualization the CCs. We have proved that the CCs for Type I/II twins are a segment of line in (λ_1, λ_3) space with $\lambda_2 = 1$ for the Cubic to Orthorhombic phase transformation, and a bounded surface in $(\lambda_1, \lambda_3, \theta)$ space with $\lambda_2 = 1$ for the Cubic to Monoclinic I/II phase transformation. By adding an extra degree of freedom θ in the Cubic to Monoclinic transformation comparing to the Cubic to Orthorhombic transformation, the exploration space for the CCs alloys are expanded massively. Figure 4 shows that in the Cubic to Monoclinic phase transformation, the CCs are very sensitive to the monoclinic angle θ . Hence, it is feasible to develop the low fatigue shape memory alloys with large transformation strain (plateau strain) in the Cubic to Monoclinic transformation.

Even though the visualization of the simplified CCs provide an intuitive way to determine the geometric compatibility conditions, the quantitative distance between the eigenvalues of the transformation stretch tensor and the simplified CCs curves/surfaces remains undeveloped, which is also worthy of future research. Another notable finding is that alloys with λ_2 approaching 1 in the Cubic to Orthorhombic transformation appear to show a linear relationship between λ_1 and λ_3 . However, the underlying physics remains unclear, and presenting an intriguing subject for future study.

Acknowledgments

References

- [1] Robert Zarnetta, Ryota Takahashi, Marcus L. Young, Alan Savan, Yasubumi Furuya, Sigurd Thienhaus, Burkhard Maaß, Mustafa Rahim, Jan Frenzel, Hayo Brunken, Yong S. Chu, Vijay Srivastava, Richard D. James, Ichiro Takeuchi, Gunther Eggeler, and Alfred Ludwig. Identification of quaternary shape memory alloys with near-

- zero thermal hysteresis and unprecedented functional stability. *Advanced Functional Materials*, 20(12):1917–1923, 2010.
- [2] Zeyuan Zhu, Mostafa Karami, Chenbo Zhang, and Xian Chen. Twinning, slip and size effect of phase-transforming ferroelectric nanopillars. *Journal of the Mechanics and Physics of Solids*, 192:105796, 2024.
- [3] C.C Koch. Experimental evidence for magnetic or electric field effects on phase transformations. *Materials Science and Engineering: A*, 287(2):213–218, 2000.
- [4] Alan Lai and Christopher A Schuh. Direct electric-field induced phase transformation in paraelectric zirconia via electrical susceptibility mismatch. *Physical review letters*, 126(1):015701, 2021.
- [5] H.E. Karaca, I. Karaman, B. Basaran, D.C. Lagoudas, Y.I. Chumlyakov, and H.J. Maier. On the stress-assisted magnetic-field-induced phase transformation in ni2mnga ferromagnetic shape memory alloys. *Acta Materialia*, 55(13):4253–4269, 2007.
- [6] Lorenza Petrini and Francesco Migliavacca. Biomedical applications of shape memory alloys. *Journal of Metallurgy*, 2011(1):501483, 2011.
- [7] Heather Holman, Minoos Naozer Kavarana, and Taufiek Konrad Rajab. Smart materials in cardiovascular implants: Shape memory alloys and shape memory polymers. *Artificial organs*, 45(5):454–463, 2021.
- [8] Ivo Stachiv, Eduardo Alarcon, and Miroslav Lamac. Shape memory alloys and polymers for mems/nems applications: Review on recent findings and challenges in design, preparation, and characterization. *Metals*, 11(3), 2021.
- [9] Junyu Chen, Liping Lei, and Gang Fang. Elastocaloric cooling of shape memory alloys: A review. *Materials Today Communications*, 28:102706, 2021.
- [10] Huilong Hou, Suxin Qian, and Ichiro Takeuchi. Materials, physics and systems for multicaloric cooling. *Nature Reviews Materials*, 7(8):633–652, 2022.
- [11] Suxin Qian and Ichiro Takeuchi. Sizing up caloric devices. *Science*, 385(6708):493–494, 2024.
- [12] Guoan Zhou, Lingyun Zhang, Zexi Li, Peng Hua, Qingping Sun, and Shuhuai Yao. Achieving kilowatt-scale elastocaloric cooling by a multi-cell architecture. *Nature*, pages 1–6, 2025.
- [13] Ashley N. Bucsek, William Nunn, Bharat Jalan, and Richard D. James. Energy conversion by phase transformation in the small-temperature-difference regime. *Annual Review of Materials Research*, 50(Volume 50, 2020):283–318, 2020.
- [14] Sooho Choo, Shivasheesh Varshney, Huan Liu, Shivam Sharma, Richard D. James, and Bharat Jalan. From oxide epitaxy to freestanding membranes: Opportunities and challenges. *Science Advances*, 10(50):eadq8561, 2024.
- [15] Vivekanand Dabade, Raghavendra Venkatraman, and Richard D James. Micromagnetics of galfenol. *Journal of Nonlinear Science*, 29:415–460, 2019.
- [16] G. R. Krishna Chand Avatar and Vivekanand Dabade. Kirchhoff’s analogy for a planar deformable ferromagnetic rod. *Journal of Applied Mechanics*, pages 1–12, 03 2025.
- [17] Ananya Renuka Balakrishna and Richard D James. Design of soft magnetic materials. *npj Computational Materials*, 8(1):4, 2022.

- [18] Richard D. James and Zhiyong Zhang. *A Way to Search for Multiferroic Materials with “Unlikely” Combinations of Physical Properties*, pages 159–175. Springer Berlin Heidelberg, Berlin, Heidelberg, 2005.
- [19] Jun Cui, Yong S. Chu, Olugbenga O. Famodu, Yasubumi Furuya, Jae. Hattrick-Simpers, Richard D. James, Alfred Ludwig, Sigurd Thienhaus, Manfred Wuttig, Zhiyong Zhang, and Ichiro Takeuchi. Combinatorial search of thermoelastic shape-memory alloys with extremely small hysteresis width. *Nature Materials*, 5(4):286–290, 2006.
- [20] Zhiyong Zhang, Richard D. James, and Stefan Müller. Energy barriers and hysteresis in martensitic phase transformations. *Acta Materialia*, 57(15):4332 – 4352, 2009.
- [21] Vijay Srivastava, Xian Chen, and Richard D. James. Hysteresis and unusual magnetic properties in the singular heusler alloy ni₄₅co₅mn₄₀sn₁₀. *Applied Physics Letters*, 97(1):014101, 2010.
- [22] Xian Chen, Vijay Srivastava, Vivekanand Dabade, and Richard D. James. Study of the cofactor conditions: Conditions of supercompatibility between phases. *Journal of the Mechanics and Physics of Solids*, 61(12):2566–2587, 2013.
- [23] Yintao Song, Xian Chen, Vivekanand Dabade, Thomas W. Shield, and Richard D. James. Enhanced reversibility and unusual microstructure of a phase-transforming material. *Nature*, 502(7469):85–88, 2013.
- [24] Christoph Chluba, Wenwei Ge, Rodrigo Lima de Miranda, Julian Strobel, Lorenz Kienle, Eckhard Quandt, and Manfred Wuttig. Ultralow-fatigue shape memory alloy films. *Science*, 348(6238):1004–1007, 2015.
- [25] Ashley N Bucsek, Grant A Hudish, Glen S Bigelow, Ronald D Noebe, and Aaron P Stebner. Composition, compatibility, and the functional performances of ternary nitix high-temperature shape memory alloys. *Shape Memory and Superelasticity*, 2(1):62–79, 2016.
- [26] Hanlin Gu, Lars Bumke, Christoph Chluba, Eckhard Quandt, and Richard D. James. Phase engineering and supercompatibility of shape memory alloys. *Materials Today*, 21(3):265 – 277, 2018.
- [27] Yunxiang Tong, Hanling Gu, Richard D. James, Wenyin Qi, Alexander V. Shuitcev, and Li Li. Novel tinicunb shape memory alloys with excellent thermal cycling stability. *Journal of Alloys and Compounds*, 782:343 – 347, 2019.
- [28] Justin Jetter, Hanlin Gu, Haolu Zhang, Manfred Wuttig, Xian Chen, Julia R. Greer, Richard D. James, and Eckhard Quandt. Tuning crystallographic compatibility to enhance shape memory in ceramics. *Phys. Rev. Materials*, 3:093603, Sep 2019.
- [29] Maike Wegner, Hanlin Gu, Richard D James, and Eckhard Quandt. Correlation between phase compatibility and efficient energy conversion in zr-doped barium titanate. *Scientific reports*, 10(1):1–8, 2020.
- [30] Edward L. Pang, Caitlin A. McCandler, and Christopher A. Schuh. Reduced cracking in polycrystalline zro₂-ceo₂ shape-memory ceramics by meeting the cofactor conditions. *Acta Materialia*, 177:230 – 239, 2019.
- [31] Y. G. Liang, S. Lee, H. S. Yu, H. R. Zhang, Y. J. Liang, P. Y. Zavalij, X. Chen, R. D. James, L. A. Bendersky, A. V. Davydov, X. H. Zhang, and I. Takeuchi. Tuning the hysteresis of a metal-insulator transition via lattice compatibility. *Nature Communications*, 11(1):3539, 2020.

- [32] Fan Feng, Paul Plucinsky, and Richard D. James. Helical miura origami. *Phys. Rev. E*, 101:033002, Mar 2020.
- [33] H. Liu, P. Plucinsky, F. Feng, and R. D. James. Origami and materials science. *Philosophical Transactions of the Royal Society A: Mathematical, Physical and Engineering Sciences*, 379(2201):20200113, 2021.
- [34] Prasanth Velvaluri, Arun Soor, Paul Plucinsky, Rodrigo Lima de Miranda, Richard D James, and Eckhard Quandt. Origami-inspired thin-film shape memory alloy devices. *Scientific reports*, 11(1):10988, 2021.
- [35] Fan Feng, Klaudia Dradrach, Michał Zmysłony, Morgan Barnes, and John S Biggins. Geometry, mechanics and actuation of intrinsically curved folds. *Soft Matter*, 20(9):2132–2140, 2024.
- [36] K. A. Bywater and J. W. Christian. Martensitic transformations in titanium-tantalum alloys. *The Philosophical Magazine: A Journal of Theoretical Experimental and Applied Physics*, 25(6):1249–1273, 1972.
- [37] Hanuš Seiner, Ladislav Straka, and Oleg Heczko. A microstructural model of motion of macro-twin interfaces in ni–mn–ga 10m martensite. *Journal of the Mechanics and Physics of Solids*, 64:198–211, 2014.
- [38] C Chu and RD James. Analysis of microstructures in cu-14.0% al-3.9% ni by energy minimization. *Le Journal de Physique IV*, 5(C8):C8–143, 1995.
- [39] Francesco Della Porta, Akira Heima, Yuri Shinohara, Hiroshi Akamine, Minoru Nishida, and Tomonari Inamura. Triplet condition: A new condition of supercompatibility between martensitic phases. *Journal of the Mechanics and Physics of Solids*, 169:105050, 2022.
- [40] Kaushik Bhattacharya et al. *Microstructure of martensite: why it forms and how it gives rise to the shape-memory effect*, volume 2. Oxford University Press, 2003.
- [41] John M Ball and Richard D James. Fine phase mixtures as minimizers of energy. In *Analysis and Continuum Mechanics*, pages 647–686. Springer, 1989.
- [42] H. Mughrabi, K. Herz, and X. Stark. Cyclic deformation and fatigue behaviour of α -iron mono-and polycrystals. *International Journal of Fracture*, 17(2):193–220, 1981.
- [43] Xian Chen, Yintao Song, Nobumichi Tamura, and Richard D. James. Determination of the stretch tensor for structural transformations. *Journal of the Mechanics and Physics of Solids*, 93:34 – 43, 2016. Special Issue in honor of Michael Ortiz.
- [44] M.J Duggin and W.A Raghinger. The nature of the martensite transformation in a coppernickel-aluminium alloy. *Acta Metallurgica*, 12(5):529 – 535, 1964.
- [45] Xiaoyue Ni, Julia R. Greer, Kaushik Bhattacharya, Richard D. James, and Xian Chen. Exceptional resilience of small-scale au30cu25zn45 under cyclic stress-induced phase transformation. *Nano Letters*, 16(12):7621–7625, 2016. PMID: 27960490.
- [46] Giovanni Zanzotto. Weak and symmetry-breaking transitions in simple lattices. *preprint*, 1996.
- [47] Richard D. James and Kevin F. Hane. Martensitic transformations and shape-memory materials. *Acta Materialia*, 48(1):197–222, jan 2000.
- [48] Kevin F. Hane. Bulk and thin film microstructures in untwinned martensites. *Journal of the Mechanics and Physics of Solids*, 47(9):1917 – 1939, 1999.

- [49] Kevin F Hane and Thomas W Shield. Microstructure in a copper–aluminium–nickel shape–memory alloy. *Proceedings of the Royal Society of London. Series A: Mathematical, Physical and Engineering Sciences*, 455(1991):3901–3915, 1999.